jove

Tetrameric Fluorescent Antigen Arrays for Single-Step Identification of Antigen-Specific B Cells

Kyle D. Apley[*,1], **J. Daniel Griffin**[*,1], **Stephanie N. Johnson**[1], **Cory J. Berkland**[1,2,3], **Brandon J. DeKosky**[1,2,3]

[1] Department of Pharmaceutical Chemistry, University of Kansas [2] Bioengineering Graduate Program, University of Kansas [3] Department of Chemical and Petroleum Engineering, University of Kansas

[*] These authors contributed equally

Corresponding Author

Brandon J. DeKosky
dekosky@ku.edu

Citation

Apley, K.D., Griffin, J.D., Johnson, S.N., Berkland, C.J., DeKosky, B.J. Tetrameric Fluorescent Antigen Arrays for Single-Step Identification of Antigen-Specific B Cells. *J. Vis. Exp.* (164), e61827, doi:10.3791/61827 (2020).

Date Published

October 20, 2020

DOI

10.3791/61827

URL

jove.com/video/61827

Abstract

Fluorescent antigen production is a critical step in the identification of antigen-specific B cells. Here, we detailed the preparation, purification, and the use of four-arm, fluorescent PEG-antigen conjugates to selectively identify antigen-specific B cells through avid engagement with cognate B cell receptors. Using modular click chemistry and commercially available fluorophore kit chemistries, we demonstrated the versatility of preparing customized fluorescent PEG-conjugates by creating distinct arrays for proteolipid protein ($PLP_{139-151}$) and insulin, which are important autoantigens in murine models of multiple sclerosis and type 1 diabetes, respectively. Assays were developed for each fluorescent conjugate in its respective disease model using flow cytometry. Antigen arrays were compared to monovalent autoantigen to quantify the benefit of multimerization onto PEG backbones. Finally, we illustrated the utility of this platform by isolating and assessing anti-insulin B cell responses after antigen stimulation ex vivo. Labeling insulin-specific B cells enabled the amplified detection of changes to co-stimulation (CD86) that were otherwise dampened in aggregate B cell analysis. Together, this report enables the production and use of fluorescent antigen arrays as a robust tool for probing B cell populations.

Introduction

The adaptive immune system plays a critical role in the progression or regression of many disease states, including autoimmunity, cancer, and infectious diseases[1]. For broad applications including the study of immunopathology or the development of new precision treatments, it is often critical to assess antigen-specific B and T cell responses underlying disease progression[2,3,4]. Major histocompatibility complex (MHC) tetramers are widely and commercially available for identifying antigen-specific T cell clones[5]. These fluorophore-labeled constructs present quadrivalent peptide-MHC complexes to avidly engage with cognate T cell

receptors for labeling applications such as microscopy and flow cytometry.

Antigens for B cell interrogation can present highly varied molecular weights, charges, and solubilities[6,7]. When using monomeric antigen as soluble B cell probes, physicochemical antigen properties may not be stabilized through complexing with the much larger, water soluble streptavidin molecule, or could present solubility issues as monomeric reagents prior to conjugation. Thus, some proteins present bioconjugation difficulties and unexpected results in practice[7,8]. Direct fluorescent dye conjugation can sometimes render constructs water insoluble and lipophilic. These direct dye-antigen compounds are susceptible to nonspecific embedding within cell membranes, confounding antigen-specific analyses[7,8,9]. Some strategies have overcome solubility challenges by coupling antigen and fluorophores with other functional groups. Cambier et al., for example, employed biotinylated insulin in its native form to engage with insulin-specific B cell receptors (BCRs) before adding fluorophore-labeled streptavidin in a stepwise fashion[10]. While this approach enabled the assessment of B cells that bind to monomeric insulin with high resolution, two labeling steps were required. A generalizable protocol for the preparation of ready-to-use polymer-based B cell probes that is readily integrated with common fluorescent antibody labeling procedures would be of benefit for furthering the study of B cells in disease.

In this protocol, we detail the production and use of fluorescent antigen arrays (FAAs) for the generalizable and single-step labeling of antigen-specific B cells for microscopy and flow cytometry experiments (**Figure 1**). Soluble antigen arrays (SAgAs) have been employed over the past decade as B cell-targeted antigen-specific immunotherapies against autoimmune diseases[11,12,13,14,15,16,17,18,19,20,21,22]. SAgAs leverage multivalent antigen display on flexible, polymeric backbones to avidly engage B cell receptors and elicit immunomodulatory effects, though their antigen-specificity provides another opportunity for probing B cells of interest when coupled to a fluorophore[23]. The polymeric backbones constituting SAgAs confer water solubility to the overall biomacromolecule and can dampen the sometimes extreme antigen characteristics that confound probe generation and staining specificity[6,24]. We have grafted numerous antigens ranging in size and complexity onto SAgA platform using modular click chemistry, which is conducive to the use of small peptide epitopes and full proteins[14,18]. Here, we demonstrate FAAs as robust antigen-specific B cell labeling tools that can be used in parallel with typical fluorescent antibody labeling. We prepared and evaluated FAAs consisting of human insulin for labeling B cells in a transgenic mouse model of Type 1 Diabetes (VH125), as well as FAAs that incorporated proteolipid protein 139-151 (PLP), a peptide epitope for experimental autoimmune encephalomyelitis (EAE), the mouse model of Multiple Sclerosis. Our intention in employing these disease models was to demonstrate the versatility of this platform, both for the modular substitution of antigens used, as well as the viability of use with peptide epitopes (PLP) and full proteins (insulin) alike. This protocol is presented with the purpose of accessibility, without extensive bioconjugation expertise required. The reagents, as well as synthesis and purification methods, are designed to be versatile and readily implemented at most research labs focused in chemistry, molecular biology, or immunology.

Protocol

All animal procedures represented in this work were approved by the Institutional Animal Care and Use Committee at the University of Kansas.

1. Antigen array synthesis (4–6 days)

1. Functionalize unmodified antigen with an alkyne handle (1 h). Add 1 equivalent insulin (100 mg, 17.4 µmol) to a 20 mL glass vial with a stir bar and dissolve in anhydrous dimethylsulfoxide (DMSO) (2 mL) with gentle heating to 40–50 °C using a heat-gun or water bath.
    1. Add 1,1,3,3-tetramethylguanidine (40.2 mg, 348.8 µmol) and 1.35 equivalents freshly prepared 78.5 mM propargyl N-hydroxysuccinimide ester (NHS-ester) stock solution in anhydrous DMSO (0.3 mL, 5.3 mg, 23.6 µmol).
    2. Stir for 30 min at room temperature then quench the reaction with 0.05% HCl (12 mL).
2. Purify the singly modified insulin-alkyne by reverse-phase liquid chromatography (4 h). Use a preparative C18 column (19 mm x 250 mm, 300 A pore size, 5 µm particle size) with a 10 min 30–40% B gradient (A, water with 0.05% trifluoroacetic acid (TFA); B, acetonitrile with 0.05% TFA) and a flow rate of 14 mL/min. The desired product elutes immediately after unmodified insulin.
    1. Evaporate acetonitrile and TFA by nitrogen gas stream or rotary evaporation under reduced pressure (650 Pascals) and rotating at 150 rpm. Freeze the aqueous solution and lyophilize to dryness. Store functionalized insulin at -20 °C under a dry atmosphere.

       NOTE: The functionalized insulin is stable for up to a year under these storage conditions.
3. Synthesize the antigen array by copper-catalyzed, azide-alkyne cycloaddition (CuAAC) (2.5 h)[22]. Add 6 equivalents insulin-alkyne (38 mg, 6.3 µmol) to a 10 mL glass vial with a stir bar and dissolve in DMSO (1.2 mL) with gentle heating.
    1. Add 50 mM sodium phosphate buffer (1.8 mL) pH 7.4, 1 equivalent 20 kDa 4-arm PEG azide (21 mg, 1.05 µmol), copper (II) sulfate pentahydrate (3.15 mg, 12.6 µmol), Tris(3-hydroxypropyltriazolylmethyl)amine (27.37 mg, 63 µmol), and sodium ascorbate (50.34 mg, 254 µmol).
    2. Stir for 2 h at room temperature then add DMSO (3 mL) to solubilize any precipitates and acidify the solution with 0.05% HCl (4 mL).
4. Purify the antigen array by reverse-phase liquid chromatography (3 h). Use a preparative C18 column (19 mm x 250 mm, 300 A pore size, 5 µm particle size) with a 10 min 20–60% B gradient (A, water with 0.05% TFA; B, acetonitrile with 0.05% TFA) and a flow rate of 14 ml/min. The desired product elutes immediately after insulin-alkyne.
    1. Evaporate acetonitrile by nitrogen gas stream or rotary evaporation under reduced pressure. Freeze the aqueous solution and lyophilize to dryness. Store at -20 °C under a dry atmosphere.

       NOTE: The insulin antigen array is highly hygroscopic. The lyophilized fibers may coalesce into a dense pellet after repeated exposure to the atmosphere. FAA properties may differ depending on the application-specific antigen used. The insulin

antigen array is stable for several months under these storage conditions.

2. Fluorophore conjugation (1–2 days)

1. Conjugate the fluorophore to the antigen array (2.5 h). Add 1 equivalent tetravalent insulin (21.7 mg, 0.5 µmol) to a 20 mL glass vial with stir bar and dissolve in DMSO (1.75 mL) with gentle heating. Add freshly prepared 100 mM carbonate buffer (8 mL) pH 9.0 and 5 equivalents of fluorescein isothiocyanate in a freshly prepared 10 mM stock solution in DMSO (0.25 ml, 0.97 mg, 2.5 µmol). Stir for 2 h in the dark at room temperature.
2. Purify the product by dialysis (24 h). Use 3.5 kDa molecular weight cutoff dialysis tubing in a stirred 5 L bucket with distilled water in the dark at room temperature. Dialyze for 24 h and change the dialysis solution every 6–12 h.
3. Freeze the dialyzed solution and lyophilize to dryness to yield the FAA. Store in the dark under a dry atmosphere at -20 °C.
   NOTE: The FAA is stable for several months under these storage conditions.

3. FAA characterization (2–4 h)

1. Analyze the products of steps 1 and 2 by sodium dodecyl sulfate-polyacrylamide gel electrophoresis according to Laemmli[25] (2 h). Prepare samples containing 5 µg of purified monovalent antigen, 20 kDa 4-arm PEG azide, antigen array, and FAA.
   1. Visualize fluorophore labeling in the FAA samples by fluorescence imaging in a gel-imager.
   2. Perform Coomassie blue staining[26] to visualize the antigen.
   3. Perform iodine staining[27] to visualize the PEG backbone. Rinse the gel in distilled water (3 x 2 min), incubate in 5% barium chloride solution (20 mL) for 10 min, rinse in distilled water (3 x 2 min), incubate in 0.1 N iodine solution (20 mL) for 1 min, then rinse in distilled water (3 x 2 min) to remove background staining before visualization.
      NOTE: To make 0.1 N iodine solution, add potassium iodide (2.0 g, 12 mmol) and iodine (1.27 g, 5 mmol) to 100 mL distilled water.
2. Calculate the degree of dye-labeling by UV-Vis spectroscopy (1 h). Dissolve a small amount of FAA at 0.1 mg/mL and record the absorbance at 280 nm and the peak absorption wavelength for the dye. Obtain the molar extinction coefficients for the antigen and the dye.
   NOTE: Some dyes are pH sensitive. Make sure to use an appropriately buffered solution like100 mM carbonate buffer with pH 8.3 when measuring the FAA absorbance to ensure the reported dye extinction coefficient is accurate.
   1. Perform the following calculation[28] where $A_{Dye,\ max\lambda}$ is the FAA absorbance at the peak absorption wavelength for the dye, $E_{Dye,\ max\lambda}$ is the molar extinction coefficient at the peak absorption wavelength for the dye, and $E_{antigen,\ 280\ nm}$ is the molar extinction coefficient for monovalent antigen at 280 nm.:
      Correction Factor (CF) = $A_{Dye,\ 280\ nm} / A_{Dye,\ max\lambda}$
      $0.25 * (A_{Dye,\ max\lambda} / E_{Dye,\ max\lambda}) * (E_{antigen,\ 280\ nm} / (A_{280\ nm} - (A_{Dye,\ max\lambda} * CF))) = dye/FAA$
3. Analyze the FAA for free dye or potential degradation products by RP-HPLC (1 h).

1. Dissolve a small amount of FAA at 1.0 mg/mL and analyze with an analytical C18 column (4.6 mm x 150 mm, 300 A pore size, 2.5 µm particle size) using a 10 min 5–95% B gradient (A, water with 0.05% trifluoroacetic acid: B, acetonitrile with 0.05% trifluoroacetic acid) with a flow rate of 1 mL/min. Set the UV-Vis detector to monitor the peak absorbance wavelength of the dye (437 nm for FITC).
   NOTE: For pH sensitive dyes, HPLC analysis in acidified solvents may require shifting the monitored wavelength from the dye's peak absorption wavelength in neutral, aqueous conditions. In 0.05% TFA, the pH is approximately 3 and the max absorption for FITC has shifted.

4. Assay development by FAA titration (3–5 h)

NOTE: FAA use for flow cytometry is presented, but the same steps can be modified for use in other formats such as immunohistochemistry or fluorescent microscopy. When applying FAAs for a new format, a new optimization assay must be completed. Mixed or isolated cell populations may be obtained through blood or lymphoid organ processing methods[23,29]. Harvest through enzymatic digestion of tissue is not recommended, as cells surface markers may be shed.

1. Suspend FAA stock to 1 mg/mL in FACS buffer (1x PBS + 5% fetal bovine serum and 0.1% sodium azide). Up to 10% DMSO can be incorporated to accelerate dissolution.
2. Obtain cells positive for antigen-specific B cells of interest and dispense into microcentrifuge tubes. Approximately 1 x 10^7 total cells will be required.
   NOTE: Splenocytes were harvested from VH125 and EAE mice according to IACUC-approved protocols at the University of Kansas for the present demonstration. Researchers may employ the methods described herein for cell samples specific to their own application and FAA preparation.
   1. Dispense 5 x 10^5 cells for titration labeling replicates (at least 3 replicates per titration).
   2. Dispense 1 x 10^5 cells for single-stain controls as well as an unstained control.
      NOTE: Antibody isotypes and fluorescence minus one control may also be used to fully validate the assay.
3. Wash cells by adding 1 mL of FACS buffer to each tube. Centrifuge at 200 x *g* for 5 min.
4. Aspirate the supernatant and resuspend cell pellets in 50 µL of FACS buffer.
5. Add CD3 and CD19 fluorescent antibodies to each sample at manufacturer recommended concentrations, as well as titrated FAA doses.
   NOTE: Fluorescent antibody working concentrations may be titrated independently to confirm the lot integrity. Appropriate FAA dose ranges will vary by application, but a good starting point is 50, 25, 10, 5, and 1 µg per sample. 1 µL of stock FAA solution equals 1 µg of dose.
6. Mix each sample well and incubate covered from light, on ice for 30 min.
7. After the incubation, wash cells by adding 1 mL of FACS buffer to each tube. Centrifuge the samples at 200 x *g* for 5 min.
8. Aspirate the supernatant and repeat the wash by adding 1 mL of FACS buffer to each tube. Centrifuge the samples at 200 x *g* for 5 min.

9. Aspirate the supernatant and resuspend the samples in 200 µL of fresh FACS buffer. Place the samples on ice and head to the cytometer.
10. Run the samples on the cytometer and collect at least 50,000 events.

5. FAA titration analysis and labeling dose optimization (1–2 h)

1. Using flow cytometry analysis software, gate for single cells.
2. On single cells, place gates for CD19+ (B cells) and CD3+ (T cells).
3. Within CD19+ and CD3+ parent populations, gate for FAA + events in the relevant fluorochrome channel.
4. Record the percentage of FAA+ events within the CD19+ and CD3+ parent populations.
5. Calculate a specificity ratio by dividing the proportion of FAA+ events in the CD19+ population (specific) by the proportion of FAA+ events in the CD3+ population (nonspecific). Specificity ratio should be maximized for successful FAA use.
6. Employ the labeling dose corresponding to the highest specificity ratio for future experiments.

Representative Results

The purified yield of insulin-alkyne (**Figure 2**, upper panel), determined by weight, typically varied from 50–65%. Yields of less than 40% were likely caused by water contamination in the anhydrous DMSO and or hydrolysis of the propargyl NHS-ester. For antigen multimerization (**Figure 1B**), the purified yield of the insulin antigen array (**Figure 2**, middle panel) varied from 60–75% and SDS-PAGE analysis confirmed the major product was the tetravalent species (**Figure 3A**). For fluorophore modification (**Figure 1C**), the purified yield of FITC 4-arm insulin FAA (**Figure 2**, lower panel) was consistently near 50%. Analysis by SDS-PAGE qualitatively confirmed dye conjugation to the tetravalent antigen array (**Figure 3A**). Analysis of FITC 4-arm insulin by HPLC at the peak absorption wavelength for FITC in acidic conditions, 437 nm, confirmed the removal of free dye (**Figure 3B**) from the material. Analysis of FITC 4-arm insulin by HPLC at 280 nm (**Supplementary Figure 1A**) showed a downfield peak shift that corresponds to the retention time of the FITC 4-arm insulin peak at 437 nm. Although the change in retention time is slight, the homogeneity of the 280 nm FITC 4-arm insulin peak supports near unity dye-labeling of the insulin antigen array. The degree of dye labeling for FITC 4-arm insulin was calculated to be 1.52 (**Supplementary Table 1**) from the absorbance spectrum (**Figure 3C**).

Rhodamine B (RhdB) insulin, FITC PLP, and RhdB 4-arm PLP FAAs were also synthesized. The purified yield of PLP antigen array was 47% after 20 h using 4.25 equivalents PLP-alkyne. The multimerization reaction was monitored by HPLC and demonstrated that using fewer equivalents of antigen-alkyne required longer reaction times. The fluorophore conjugation reactions were performed for all FAAs in identical conditions. The degree of dye-labeling was calculated for each FAA (**Supplementary Table 1**) from their respective absorbance spectrums (**Supplementary Figure 3**) and purity was evaluated by HPLC (**Supplementary Figure 1** and **Supplementary Figure 2)** The degree of dye-labeling for RhdB insulin, FITC PLP, and RhdB 4-arm PLP was 0.25, 2.54, and 0.1, respectively. The low degree of dye-labeling for RhdB insulin and RhdB PLP, as calculated from the absorbance spectrum, was unexpected and conflicts with the near-complete conversion of insulin and PLP antigen arrays to a new species observed by HPLC (**Supplementary Figure**

1B and **Supplementary Figure 2B**). The HPLC spectra for each FAA (**Supplementary Figure 1** and **Supplementary Figure 2**) demonstrated the purity of the final product. All FAAs besides the RhdB 4-arm insulin were entirely free of non-conjugated dye. The purified RhdB 4-arm insulin had free dye present that contributed to 20% of the area under the curve in the 555 nm spectra. While this amount of free dye did not hamper its utility in flow cytometry assays, dialysis should be continued to fully remove the free dye in order to calculate the degree of labeling by UV-vis spectroscopy.

In the examples provided, FAA variants were constructed using human insulin and PLP. Human insulin is the cognate antigen for VH125 NOD mouse splenocytes, a transgenic line harboring 1-3% insulin-specific B cells (IBCs) within the total B cell pool[30]. PLP is an encephalitogenic peptide epitope used to induce EAE, a murine model of multiple sclerosis. Antibodies are generated against the PLP epitope in this model, indicating a B cell response[31]. These models were each employed to demonstrate FAA utility for full protein antigens and antigenic epitopes alike.

Assay development by FAA titration was carried out for FITC 4-arm insulin and RhdB 4-arm PLP in their cognate cell populations (**Figure 4**, **Supplementary Figures 4–7**). VH125 mice were bred at the University of Kansas under institutional animal care and use (IACUC) guidelines and splenocytes were harvested from a male at approximately 30 weeks of age. EAE cells were obtained from 4–6-week-old female SJL/J mice 14 days after inducing the disease under IACUC-approved guidelines. Staining differences were appreciable between CD19+FAA+ IBCs and CD3+FAA+ T cells in VH125 splenocytes (**Figure 4**). A distinct FAA population was evident among CD19+ cells, while nonspecific FAA+ staining among CD3+ T cells was more of a smear that was minimized at low labeling dose (**Figure 4A,B**). By compiling specificity ratios at each tested dose, we showed that the specificity was highest at a labeling concentration of 0.02 mg/mL (**Figure 4C**). Similar success was harnessed for probing PLP-specific B cells in the EAE model, where a 0.1 mg/mL labeling dose was optimized (**Supplementary Figure 6** and **Supplementary Figure 7D**). However, PLP-specific staining in EAE splenocytes was not as distinct as was observed with insulin-specific staining in the VH125 cells.

The benefit of antigen multimerization on a polymeric backbone was assessed by comparing IBC staining using FITC 4-arm insulin compared to monovalent RhdB insulin in the same flow cytometry panel at 0.02 mg/mL each (**Figure 4D**, **Supplementary Figure 8**). Parallel analysis uncovered that 4-arm antigen provided higher staining of the IBC population that was better separated from the FAA negative cells for improved specificity (**Supplementary Figure 8**). These data showed that roughly half of IBCs would have been unidentified if RhdB insulin was used alone, despite a higher molar amount of the monovalent antigen at 0.02 mg/mL.

After titrating insulin and PLP FAAs for flow cytometry, we conducted a mock antigen stimulation assay to assess robustness for practical application using FITC-labeled FAAs (**Figure 5**, **Supplementary Figures 9–11**). After challenging VH125 or EAE splenocytes for 24 hours with or without 10 µg/mL of cognate antigen (insulin or PLP, respectively), FAA+ populations were gated on $FITC_{hi}$+ scatter (**Supplementary Figures 9–10**). Differences in antigen-specific B cell prevalence could be assessed directly (**Figure 5A**, **Supplementary Figure 11A.**), but the most notable use for FAAs was evident in analyzing cell phenotype changes within antigen-specific B cell populations (**Figure 5B,C,** and **Supplementary Figure**

11B,C), revealing statistically significant cellular changes that are obscured during analysis of splenocyte population data. In this application demonstration, CD86 (costimulation) was assessed as a model biomarker that responds to antigen stimulation (commercially available fluorescent antibodies were employed for the analysis)[22,32]. CD86 is upregulated when B cell receptors engage with cognate autoantigen, so we hypothesized that changes in this marker would be enhanced in antigen-specific B cells after antigen challenge. Mean fluorescence intensity (MFI) was slightly elevated upon antigen challenge in VH125 and EAE splenocytes, but these increases were concentrated in antigen-specific B cells (**Figure 5B**, **Supplementary Figure 11B**). Further, antigen-specific B cells were consistently observed to present higher levels of the CD86 costimulatory marker than the rest of the B cell pool. These data validated FAAs as powerful tools for probing disease-relevant changes in adaptive immune-mediated disorders.

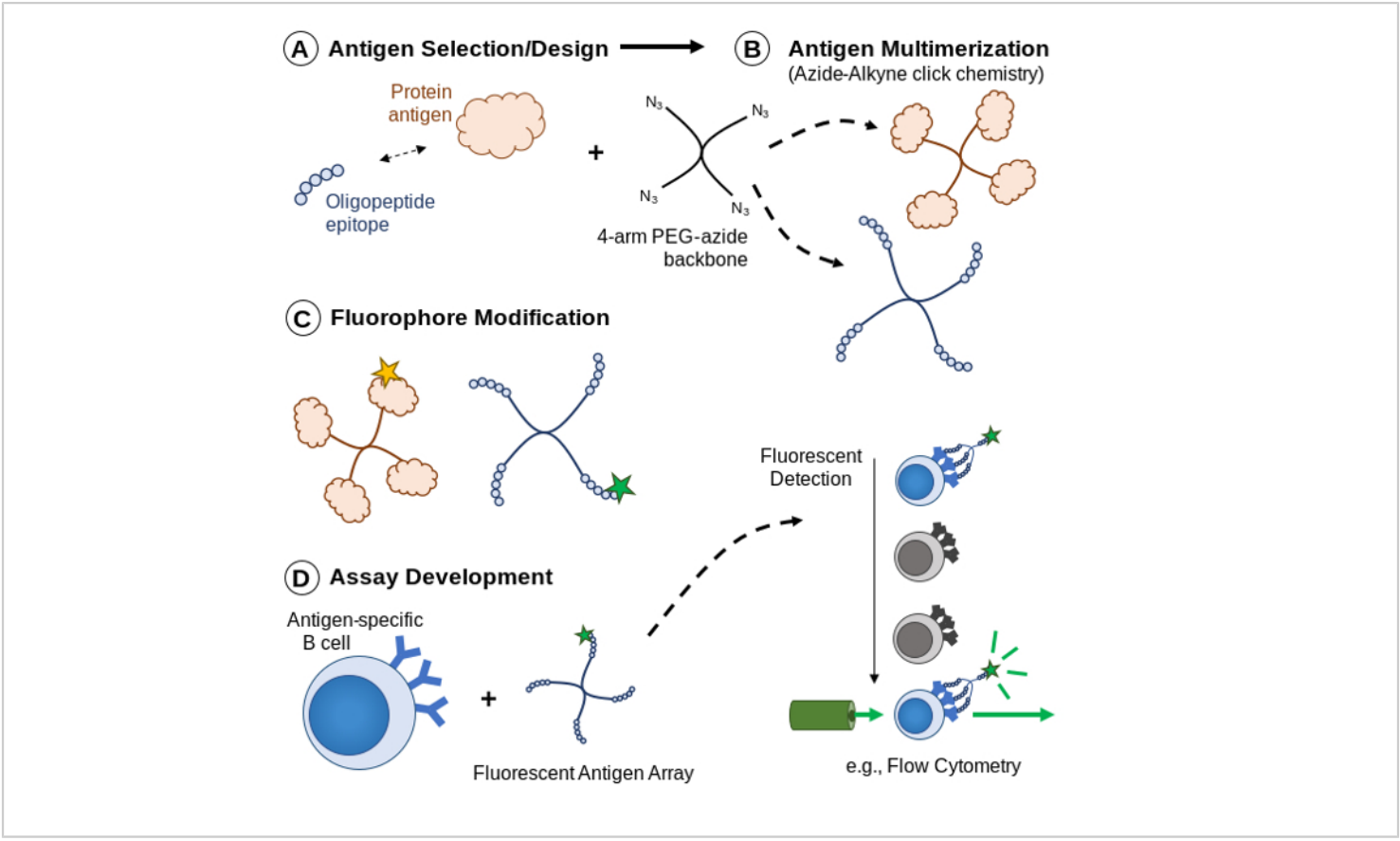

Figure 1: Overview of custom FAA generation as fluorescent B cell probes. (**A**) The desired protein or peptide epitopes are selected for antigen-specific B cell detection. (**B**) Copper (I) catalyzed azide-alkyne cycloaddition facilitates the quadrivalent multimerization of antigen onto 4-arm PEG polymer backbones. (**C**) 4-arm PEG with conjugated antigens are modified with fluorophore at an average of one equivalent per polymer backbone. (**D**) Purified fluorescent antigen arrays are titrated and validated in biological assays to analytically interrogate antigen-specific B cells. Please click here to view a larger version of this figure.

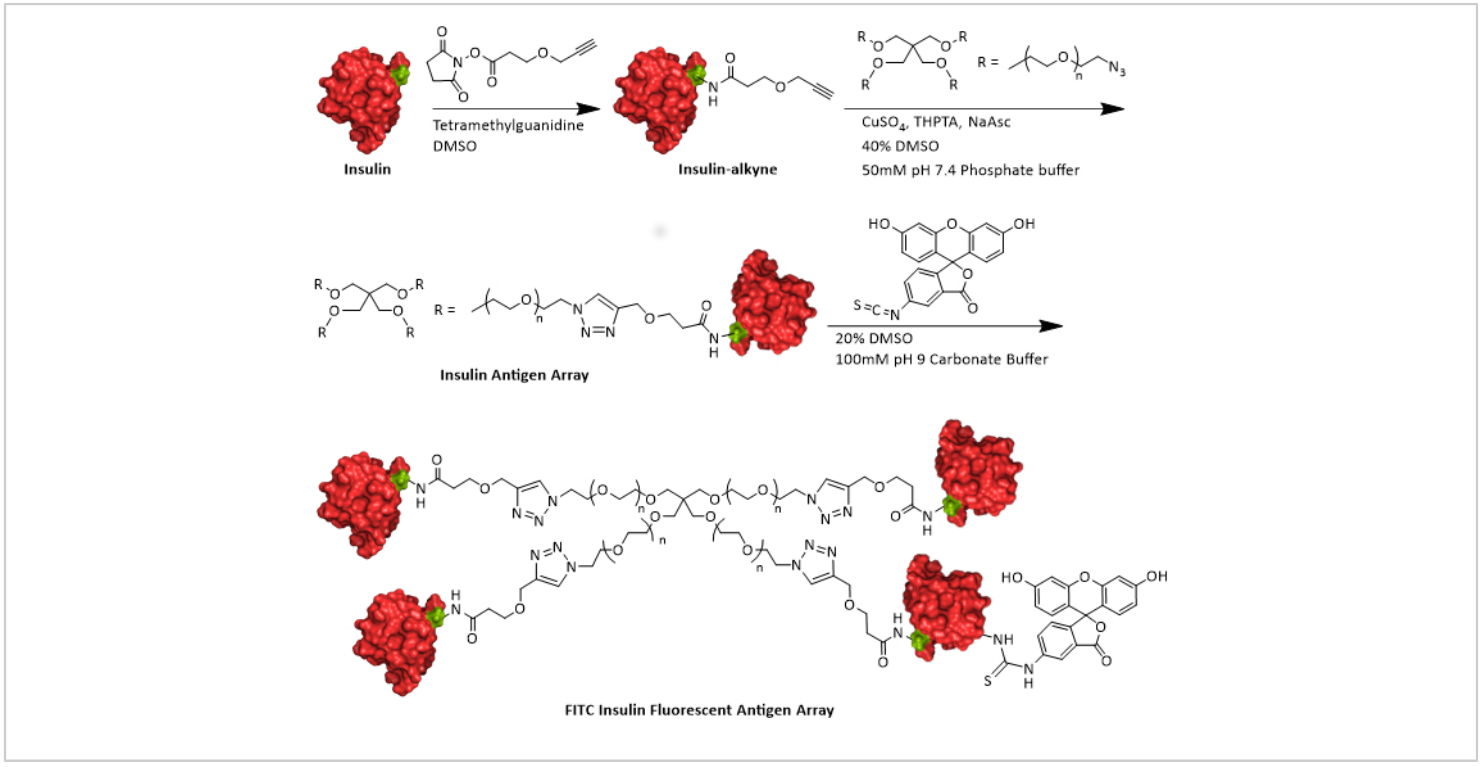

Figure 2: Reaction synthesis pathways for generating FAAs. These reaction conditions support a broad range of protein and fluorophore conjugates. The synthesis of FITC-insulin FAAs is shown as an example. Please click here to view a larger version of this figure.

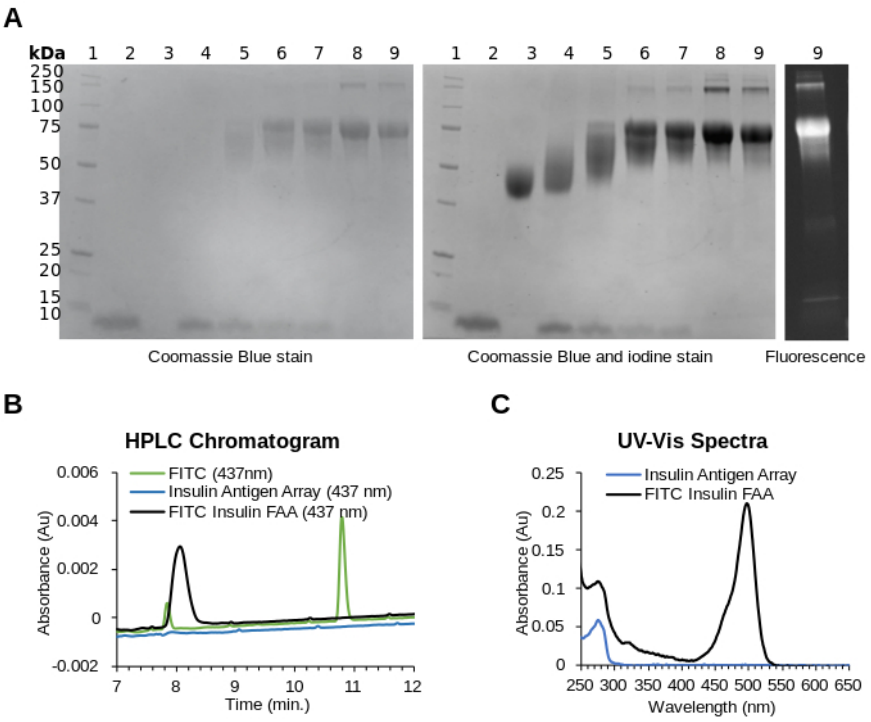

Figure 3: Synthesis and purification results for insulin FAAs. The insulin antigen array and FITC insulin FAA were analyzed for purity and characterized to determine the degree of dye-labeling. (**A**) The samples analyzed by SDS-PAGE are: 1, ladder; 2, insulin-alkyne; 3, 20 kDa 4-arm PEG azide; 4, 1.3. t = 1 min; 5, 1.3. t = 10 min; 6, 1.3. t = 60 min; 7, 1.3. t = 120 min; 8, purified insulin antigen array; 9, FITC 4-arm insulin FAA. Gels were stained with (left) Coomassie Blue to visualize protein, (middle) Coomassie Blue and iodine to visualize protein and PEG, and (right) fluorescence imaging to visualize dye. (**B**) FITC 4-arm insulin FAA was analyzed by HPLC at 437 nm to determine purity. (**C**) FITC 4-arm insulin FAA (0.01 mg/mL) and insulin antigen array (0.01 mg/mL) were analyzed by UV-Vis spectroscopy to calculate the degree of dye-labeling.

Please click here to view a larger version of this figure.

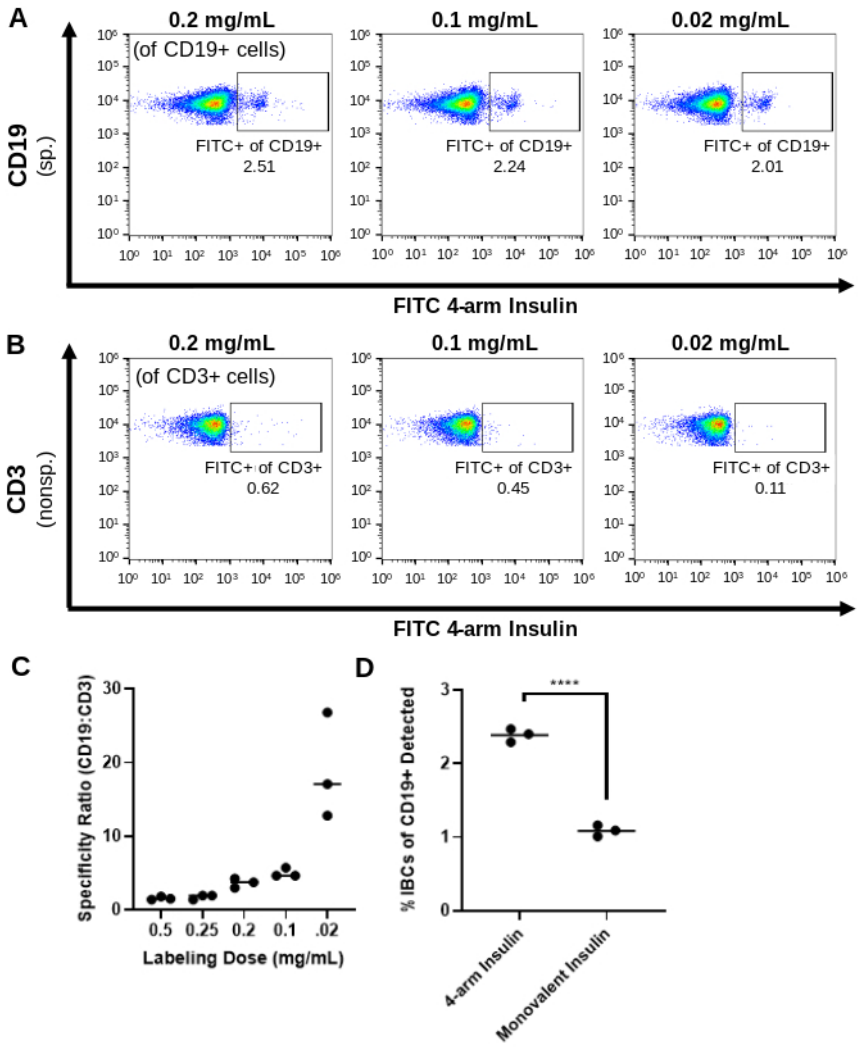

Figure 4: Representative results for titrating FAAs for flow cytometry assay development. (**A**) Specific positive events were gated among B cells (CD19+) for a range of labeling titrations. (**B**) The same analysis was performed by gating in a T cells (CD3+) that nonspecifically bound FAAs. (**C**) FAA+ of CD19+ (specific) events were divided by FAA+ of CD3+ (nonspecific) events at each titration to yield a specificity ratio, which was optimized for further application-specific FAA use. (**D**) Antigen-specific B cell labeling was compared between FAAs and monovalent fluorescent antigen. Results were compared using a two-tailed, unpaired t test (n = 3/group, *p < 0.05, **p < 0.01). Please click here to view a larger version of this figure.

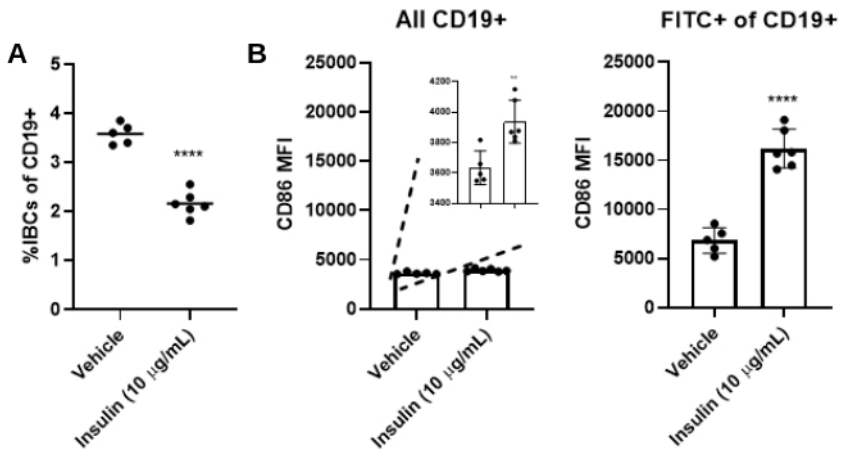

Figure 5: Demonstration of FAA screening in an animal model of Type I diabetes. Transgenic VH125 splenocytes were incubated with 10 µg/mL of insulin or media alone (vehicle) for 24 h. (**A**) FAAs were used to quantify insulin-specific B cells among the CD19+ population between the treatments. (**B**) Gating on insulin-specific B cells (right) enabled the quantification of CD86 MFI in comparison to aggregate CD19+ data (left). All statistical analyses were conducted using two-tailed, unpaired t tests (n = 6/group, *p < 0.05, **p < 0.01, ***p < 0.001, ****p < 0.0001). Please click here to view a larger version of this figure.

Supplementary Figure 1: HPLC analysis of 4-arm insulin FAAs to evaluate dye conjugation and purity. (**A**) HPLC chromatograms of FITC 4-arm insulin FAA at 437 nm (upper) and at 280 nm (lower). (**B**) HPLC chromatograms of RhdB 4-arm insulin FAA at 555 nm (upper) and at 280 nm (lower). Please click here to download this figure.

Supplementary Figure 2: HPLC analysis of 4-arm PLP FAAs to evaluate dye conjugation and purity. (**A**) HPLC chromatograms of FITC 4-arm PLP FAA at 437 nm (upper) and at 280 nm (lower). (**B**) HPLC chromatograms of RhdB 4-arm PLP FAA at 555 nm (upper) and at 280 nm (lower). Please click here to download this figure.

Supplementary Figure 3: Analysis of FAAs by UV-Vis spectroscopy to calculate the degree of dye labeling for each FAA. Please click here to download this figure.

Supplementary Table 1: Constants values used to calculate the degree of dye labeling for each FAA. Please click here to download this table.

Supplementary Figure 4: Representative gating for the flow cytometry studies. Examples of splenocyte gating (left), singlet isolation (center), and CD19/CD3 gating (right) are provided. Please click here to download this figure.

Supplementary Figure 5: Representative titration data for FITC 4-arm insulin in VH125 splenocytes are presented across the full range of concentrations from 0.5 (left) to 0.02 (right) mg/mL in CD19+ (upper) and CD3+ (lower) cells. Please click here to download this figure.

Supplementary Figure 6: Representative titration results for rhodamine 4-arm PLP in EAE splenocytes are presented across the full range of concentrations from

0.5 (left) to 0.02 (right) g in CD19+ (upper) and CD3+ (lower) cells. Please click here to download this figure.

Supplementary Figure 7: Representative specificity ratio analysis among FAAs for VH125 and EAE splenocytes. (**A**) FITC 4-arm insulin labeled cells as a percentage of parent CD19+ (left) or CD3 (right) VH125 cells. (**B**) Specificity ratio (FAA+ of CD19+/FAA+ of CD3+) was calculated for each labeling dose. (**C**) Rhodamine 4-arm PLP labeled cells as a percentage of parent CD19+ (left) or CD3 (right) EAE cells. (**D**) Specificity ratio (FAA+ of CD19+/FAA+ of CD3+) was calculated for each labeling dose. (n = 3/group) Please click here to download this figure.

Supplementary Figure 8: Monovalent antigen labeling was directly compared with FAA for specific (left) and nonspecific (right) binding (n = 3). Quadrant 3 is encompassed on the left plot by a blue box to highlight the population of IBCs that is identified by FAAs, but not monovalent insulin. Please click here to download this figure.

Supplementary Figure 9: Representative flow cytometry gating used for splenocyte assays. (**A**) FAA+ (FITC+) cells were identified among vehicle-treated (left) and insulin-treated (right) B cells (VH125). (**B**) FAA+ (FITC+) cells were identified among vehicle-treated (left) and PLP-treated (right) B cells (EAE) (n = 6/group). Please click here to download this figure.

Supplementary Figure 10: Single-stain fluorescent labeling. Single-stain fluorescent labeling control samples for the FAA flow cytometry assay shown in Fig. 5 and Supp. Fig. 11. From left to right 5,000 events were collected for unstained splenocytes, and single stain A647-CD19, FITC-FAA, PE/Cy7-CD3, and PE-CD86 splenocytes. Scatter plots are provided signal comparison in the PE/Cy7 and PE channels (upper), and A647 vs. FITC is provided with overlaid FITC+ and FITC- plots to verify minimal spectral overlap between the critical CD19 and FAA markers in our assay (lower). Please click here to download this figure.

Supplementary Figure 11: Demonstration of FAA practical utility. EAE splenocytes were challenged with 10 µg/mL of PLP or media alone (vehicle) for 24 h. (**A**) FAAs were used to quantify PLP-specific B cells among the CD19+ population between the treatments. (**B**) Gating on PLP-specific B cells (right) enabled the quantification of CD86 MFI in PLP-specific B cells compared to aggregate CD19+ B cell data (left). All statistical analyses were conducted using two-tailed, unpaired t tests (n = 6/group, *p < 0.05, **p < 0.01) Please click here to download this figure.

Discussion

We developed a protocol (**Figure 1**) to construct customized FAAs for identifying antigen-specific B cells, simplifying the generation of B cell probes for difficult antigen targets. We selected 4-arm PEG polymers with terminal azide groups as a facile substrate for building FAAs, as PEG confers water solubility while the functional azide handles enable simple click conjugation reactions[33]. The defined number of functional handles (4 arms) is conducive to simplified chemical antigen conjugation because antigen can be used in molar excess to circumvent the need for rigorous reaction optimizations. Researchers building FAAs of their own should consider the need for alkyne functionality when designing antigens. Oligopeptide epitopes can be custom ordered or synthesized with homopropargyl handles from synthetic peptide suppliers. NHS chemistry can also be employed to modify larger protein antigens with alkyne functional groups[18]. If the NHS-esterification in Step 1.1. does not proceed, a likely culprit may be hydrolysis of the NHS-

ester. This event can occur if the NHS-ester is not properly stored under a dry atmosphere, or during the reaction if the anhydrous DMSO is contaminated with water. If the copper-catalyzed, azide-alkyne cycloaddition in Step 1.3. fails to produce a tetravalent antigen array, potential solutions include increasing the concentration of reactant antigen or heating to 37 °C. If the reaction fails to proceed at all, check that the antigen is free from metal-chelating excipients and oxidizing agents.

We selected a two-step synthesis reaction for FAAs, consisting first of complete antigen occupancy on the PEG backbone followed by modification of one antigen with a fluorophore of choice. This format simplifies antigen conjugation chemistry, and is conducive to generalized protein labeling chemistries used in commercially-available kits[34]. Antigen modification of some molecules using random chemical conjugation could occlude some antigenic sites, however even bivalent or trivalent ligand presentation markedly increases binding avidity[35,36]. Ideally, there will be 1 fluorophore per FAA. Varying dye equivalents, antigen array concentrations, and reaction times can be useful to optimize the procedure for specific antigens. If the fluorophore conjugation in Step 2 performs poorly, confirm the carbonate buffer and fluorophore stock solutions were prepared immediately before use, as the pH of carbonate buffers can drift substantially and isothiocyanate or NHS-ester fluorophores will hydrolyze in DMSO if trace water is present. If researchers seek to maximize functional antigen valency, further antigen design variance may be considered, including the addition of charged amino acid residues like lysine in the custom synthesis of peptide epitopes, or through recombinant engineering of protein antigens. A wide variety of fluorophores and dye labeling kits may be selected by researchers based on compatibility with other fluorochromes in assay panels.

A final consideration for synthesis and characterization of FAAs is the use of organic solvents. In the protocol above, DMSO may be omitted from Step 1.3 (antigen multimerization via CuAAC) and Step 2.1 (fluorophore conjugation) without issue, as the solvent is only used to aid in antigen or dye dissolution when poor solubility is observed. For Step 1.1. (antigen functionalization with alkyne handle) switching to a buffered aqueous solution will require increased equivalents of propargyl NHS-ester, as hydrolysis of the NHS-ester will compete with conjugation. Additionally, a more heterogenous product will result as the described reaction conditions promote acylation of the single lysine on insulin over the two n-termini[37]. For larger protein antigens that are unstable in organic solvents, amine-selective acylation reactions performed at neutral pH will favor modification of the n-terminal amine, as n-terminal amines possess lower pKas than lysine side-chains[38]. Further, alkyne functionalized protein antigens may be purified by ion-exchange chromatography to avoid exposure to organic solvents. Purification of antigen arrays containing sensitive antigens can be conducted similarly, or dialysis may be used when oligopeptide epitopes under 2,000 Da are used.

In this report we fabricated 4-arm PEG constructs with either PLP or insulin to demonstrate versatility using peptide and protein antigens (**Figure 3**, **Supplementary Figures 1–3**). We grafted each variant to either FITC or RhdB dyes to also illustrate fluorochrome customizability (**Figure 3**, **Supplementary Figures 1–2**). After titrating FAA variants for exposure to cell populations (FITC 4-arm insulin into VH125 splenocytes, RhdB 4-arm PLP into EAE splenocytes), the benefits of FAAs over monovalent antigen were readily

apparent. While VH125 B cells labeled with a clear FAA+ population (**Figure 4**), FAA+ B cells from the EAE model were less distinct. This difference may have been due to the lower affinity and/or lower prevalence of PLP-specific B cells in splenocytes from the EAE disease model, which were harvested only 14 days from disease induction[39]. This difference also highlights the fact that the fraction of labeled B cells will differ based on disease model and target BCR affinities. Nonetheless, gating on the "high" staining population in EAE splenocytes led to similar phenotypic B cell changes as with the VH125 analysis when FITC FAAs were used for both models (**Figure 5**, **Supplementary Figure 11**). The clear benefit to FAAs over fluorophore-labeled monovalent antigen was observed as a higher separation of FAA- and FAA+ populations, likely from the enhanced avidity conferred by multivalent antigen presentation (**Figure 4C**, **Supplementary Figure 8**). One potential limitation of the FAA approach is that covalent ligation reactions may prove difficult with entities of very high molecular weight or structural complexity. Peptide epitopes are often ligated with ease into FAAs due to the peptide's molecular simplicity, but linear peptides cannot present conformational B cell epitopes. The use of full protein antigens on FAAs, as we have shown here, enables the specific labeling of conformation-specific B cell receptors.

FAAs are produced by a two-step conjugation scheme that yields ready-to-use fluorescent constructs that can be aliquoted and stored for use. Compared to other methods such as the subsequent labeling of biotinylated antigen plus streptavidin in series, our front-loaded production blueprint may cumulatively save time during antibody labeling, as FAAs may be used in parallel during labeling with other fluorescent antibodies in a single step. While the use of FAAs was demonstrated in murine cells for this work, the principles should likewise apply in human applications, though application-specific assay development and optimization should be conducted.

Disclosures

CJB is co-founder of Orion Bioscience, Inc., a company licensing the SAgA technology for investigating its therapeutic uses.

This report is based upon work supported by the National Science Foundation Graduate Research Program under Grant No. 1946099. Any opinions, findings, and conclusions or recommendations expressed in this material are those of the authors and do not necessarily reflect the views of the National Science Foundation.

Acknowledgments

We thank Colette Worcester for help with data collection. This work was supported by the PhRMA Foundation (JDG), the National Science Foundation Graduate Research Fellowship Program (KDA), and by NIH grants R21AI143407, R21AI144408, and DP5OD023118.

References

1. Murphy, K., Weaver, C. *Janeway's Immunobiology.* Garland Science. (2016).
2. Sospedra, M., Martin, R. *Immunology of Multiple Sclerosis*, Seminars in Neurology, Thieme Medical Publishers. 115-127. (2016).
3. Knutson, K. L., Disis, M. Tumor antigen-specific T helper cells in cancer immunity and immunotherapy. *Cancer Immunology, Immunotherapy.* **54** (8), 721-728 (2005).
4. Rivino, L. et al. Hepatitis B virus–specific T cells associate with viral control upon nucleos (t) ide-analogue therapy

discontinuation. *The Journal of Clinical Investigation.* **128** (2), 668-681 (2018).

5. Constantin, C. M., Bonney, E. E., Altman, J. D., Strickland, O. L. Major histocompatibility complex (MHC) tetramer technology: an evaluation. *Biological Research For Nursing.* **4** (2), 115-127 (2002).
6. Griffin, J. D., Song, J. Y., Sestak, J. O., DeKosky, B. J., Berkland, C. J. Linking autoantigen properties to mechanisms of immunity. *Advanced Drug Delivery Reviews.* (2020).
7. Moody, M. A.; Haynes, B. F. Antigen-specific B cell detection reagents: use and quality control. *Cytometry A.* **73** (11), 1086-1092 (2008).
8. Boonyaratanakornkit, J.; Taylor, J. J. Techniques to study antigen-specific B cell responses. *Frontiers in Immunology.* **10** (1694), (2019).
9. Newman, J., Rice, J. S., Wang, C., Harris, S. L., Diamond, B. Identification of an antigen-specific B cell population. *Journal of Immunological Methods.* **272** (1), 177-187 (2003).
10. Smith, M. J. et al. Silencing of high-affinity insulin-reactive B lymphocytes by anergy and impact of the NOD genetic background in mice. *Diabetologia.* **61** (12), 2621-2632 (2018).
11. Griffin, J. D. et al. Acute B-cell inhibition by soluble antigen arrays is valency-dependent and predicts immunomodulation in splenocytes. *Biomacromolecules.* **20** (5), 2115-2122 (2019).
12. Hartwell, B. L. et al. Antigen-specific binding of multivalent soluble antigen arrays induces receptor clustering and impedes B cell receptor mediated signaling. *Biomacromolecules.* **17** (3), 710-722 (2016).
13. Hartwell, B. L., Pickens, C. J., Leon, M., Berkland, C. Multivalent soluble antigen arrays exhibit high avidity binding and modulation of B cell receptor-mediated signaling to drive efficacy against experimental autoimmune encephalomyelitis. *Biomacromolecules.* **18** (6), 1893-1907 (2017).
14. Hartwell, B. L. et al. Soluble antigen arrays disarm antigen-specific B cells to promote lasting immune tolerance in experimental autoimmune encephalomyelitis. *Journal of Autoimmunity.* **93,** 76-88 (2018).
15. Hartwell, B. L. et al. Molecular dynamics of multivalent soluble antigen arrays support a two-signal co-delivery mechanism in the treatment of experimental autoimmune encephalomyelitis. *Molecular Pharmaceutics.* **13** (2), 330-343 (2016).
16. Kuehl, C. et al. Pulmonary administration of soluble antigen arrays is superior to antigen in treatment of experimental autoimmune encephalomyelitis. *Journal of Pharmaceutical Sciences.* **106** (11), 3293-3302 (2017).
17. Leon, M. A. et al. Soluble antigen arrays displaying mimotopes direct the response of diabetogenic T Cells. *ACS Chemical Biology.* **14** (7), 1436-1448 (2019).
18. Leon, M. A. et al. Soluble antigen arrays for selective desensitization of Insulin-Reactive B cells. *Molecular Pharmaceutics.* **16** (4), 1563-1572 (2019).
19. Sestak, J. O., Fakhari, A., Badawi, A. H., Siahaan, T. J., Berkland, C. Structure, size, and solubility of antigen arrays determines efficacy in experimental autoimmune encephalomyelitis. *The AAPS Journal.* **16** (6), 1185-1193 (2014).

20. Sestak, J. O. et al. Codelivery of antigen and an immune cell adhesion inhibitor is necessary for efficacy of soluble antigen arrays in experimental autoimmune encephalomyelitis. *Molecular Therapy-Methods & Clinical Development.* **1,** 14008 (2014).
21. Thati, S. et al. Routes of administration and dose optimization of soluble antigen arrays in mice with experimental autoimmune encephalomyelitis. *Journal of Pharmaceutical Sciences.* **104** (2), 714-721 (2015).
22. Johnson, S. N. et al. Multimeric insulin desensitizes insulin-specific B cells. *ACS Applied Bio Materials.* (2020).
23. Griffin, J. D. et al. Antigen-specific immune decoys intercept and exhaust autoimmunity to prevent disease. *Biomaterials.* **222,** 119440 (2019).
24. Hartwell, B. L. et al. Multivalent nanomaterials: learning from vaccines and progressing to antigen-specific immunotherapies. *Journal of Pharmaceutical Sciences.* **104** (2), 346-361 (2015).
25. Laemmli, U. K., Cleavage of structural proteins during the assembly of the head of bacteriophage T4. *Nature.* **227** (5259), 680-685 (1970).
26. Simpson, R. J. Staining proteins in gels with coomassie blue. *CSH Protocols.* **2007,** pdb. prot4719-pdb. prot4719 (2007).
27. Moosmann, A., Müller, E., Böttinger, H. Purification of PEGylated proteins, with the example of PEGylated lysozyme and PEGylated scFv. *Methods Molecular Biology.* **1129,** 527-538 (2014).
28. Haugland, R. P., Coupling of monoclonal antibodies with fluorophores. In *Monoclonal Antibody Protocols*, Davis, W. C., Ed. Humana Press: Totowa, NJ. 205-221 (1995).
29. Martin, T. J., Whalen, M. M. Exposures to the environmental toxicants pentachlorophenol (PCP) and dichlorodiphenyltrichloroethane (DDT) modify secretion of interleukin 1-beta (IL-1β) from human immune cells. *Archives of Toxicology.* **91** (4), 1795-1808 (2017).
30. Felton, J. L., Maseda, D., Bonami, R. H., Hulbert, C., Thomas, J. W. Anti-insulin B cells are poised for antigen presentation in type 1 diabetes. *The Journal of Immunology.* **201** (3), 861-873 (2018).
31. Griffin, J. D. et al. Tocopherol emulsions as functional autoantigen delivery vehicles evoke therapeutic efficacy in experimental autoimmune encephalomyelitis. *Molecular Pharmaceutics.* **16** (2), 607-617 (2019).
32. Yarkoni, Y., Getahun, A., Cambier, J. C. Molecular underpinning of B-cell anergy. *Immunology Reviews.* **237** (1), 249-263 (2010).
33. Pickens, C. J., Johnson, S. N., Pressnall, M. M., Leon, M. A., Berkland, C. J. Practical considerations, challenges, and limitations of bioconjugation via azide–alkyne cycloaddition. *Bioconjugate Chemistry.* **29** (3), 686-701 (2017).
34. Song, J. Y. et al. Glatiramer acetate persists at the injection site and draining lymph nodes via electrostatically-induced aggregation. *Journal of Controlled Release.* **293**, 36-47 (2019).
35. van Dongen, M. A. et al. Avidity mechanism of dendrimer–folic acid conjugates. *Molecular Pharmaceutics.* **11** (5), 1696-1706 (2014).
36. Hudson, P. J., Kortt, A. A. High avidity scFv multimers; diabodies and triabodies. *Journal of Immunological Methods.* **231** (1), 177-189 (1999).

37. Baker, J. C. et al. Selective acylation of epsilon-amino groups. Google Patents: (2003).

38. Grimsley, G. R., Scholtz, J. M., Pace, C. N. A summary of the measured pK values of the ionizable groups in folded proteins. *Protein Science.* **18** (1), 247-251 (2009).

39. Fesel, C., Coutinho, A. Serum IgM repertoire reactions to MBP/CFA immunization reflect the individual status of EAE susceptibility. *Journal of Autoimmunity.* 14 (4), 319-324 (2000).